Urban airflow: what drone pilots need to know

Barber, Hali; Wall, Alanna; National Research Council of Canada. Aerospace Research Centre

Publisher's version / Version de l'éditeur:
https://doi.org/10.4224/40002000
Laboratory Technical Report (National Research Council of Canada. Aerospace. Aerodynamics Laboratory); no. LTR-AL-2020-0075, 2021-01-29

UNPROTECTED

NRC·CNRC

Urban Airflow: What Drone Pilots Need to Know

LTR-AL-2020-0075
January 29, 2021

Hali Barber, Alanna Wall

Aerospace Research Centre

National Research Council Canada
Conseil national de recherches Canada

Canada

AERODYNAMICS LABORATORY

Urban Airflow: What Drone Pilots Need to Know

Report No.: LTR-AL-2020-0075

Date: January 29, 2021

Authors: Hali Barber, Alanna Wall

Classification:	Unprotected	**Distribution:**	Unlimited
For:	Transport Canada		
Project #:	A1-017743		
Submitted by:	Michael Benner, **Director of Research and Development, Aerodynamics**		
Approved by:	Mouhab Meshreki, **Director General (Acting), NRC Aerospace Research Centre**		

Pages:	26	**Copy No:**	
Figures:	29	**Tables:**	3

Executive Summary

Within an urban environment, a remotely piloted aircraft system (RPAS) flight plan must account for restrictions in pathways, loss of visual line of sight due to buildings, a limited number of emergency safe landing locations, and avoidance of populated areas. Adding to the complexity of navigating around the city structures are urban wind characteristics caused by interactions between wind and the structures. For RPAS to operate safely in an urban environment, the effects that various forms of airflow have on their controllability and hence flight path, may be of concern.

Without detailed knowledge of specific airflow patterns for a Canadian city or the effect that the airflow has on a specific RPAS, a starting point for preparing RPAS users for urban wind conditions is to provide awareness of types of urban airflow and where/when that airflow type may occur.

To support Transport Canada (TC) promotion of safe operation of RPAS within the urban environment during the early stage of the regulatory development process, an RPAS user awareness video (Urban Airflow: What Drone Pilots Need to Know) on urban airflow characteristics was provided to TC by the NRC in both English and French languages.

The specific urban airflow characteristics expected to challenge RPAS operation control and limits include; speed (S), direction (D), shear (S), turbulence (T) and vorticity (V). These airflow characteristics define the acronym used in the video - SDSTV.

The generalized magnitudes and descriptions of urban airflow features in the video include:

(S):

- Wind speed at 122 m (400 ft, maximum altitude for a small RPAS) equals $\underline{1.5 \times U_{10}}$, where U_{10} is the mean hourly wind speed reported by a weather station at a height of 10 m (33 ft) from a nearby airport.
- Wind speed estimations at heights <u>below 122 m</u> (400 ft) and within the urban environment (reference table).
- Wind speed may vary at any height by <u>18 km/h</u> (10 knots) in the urban environment.
- Wind speed may <u>double</u> within constricted paths - venturi effect.

(D):

- Wind direction changes significantly around tall buildings forming currents of updraft, downdraft, horizontal flow and flow reversal.

(S):

- Wind shear layers develop at building corners and consist of a <u>strong velocity gradient</u>.

- Wind shear layers flap inward and outward.

(T):

- Atmospheric turbulence intensity can be up to 40% within the urban environment.

(V):

- Building-induced vortices can shed in a side-to-side sequence where the vortex size is similar to the building width.
- Building-induced vortices with a horizontal trajectory can develop at rooftop corners.

Figure 2.13 is a copy of the image at the conclusion of the video. The image summarizes the urban airflow characteristics, SDSTV.

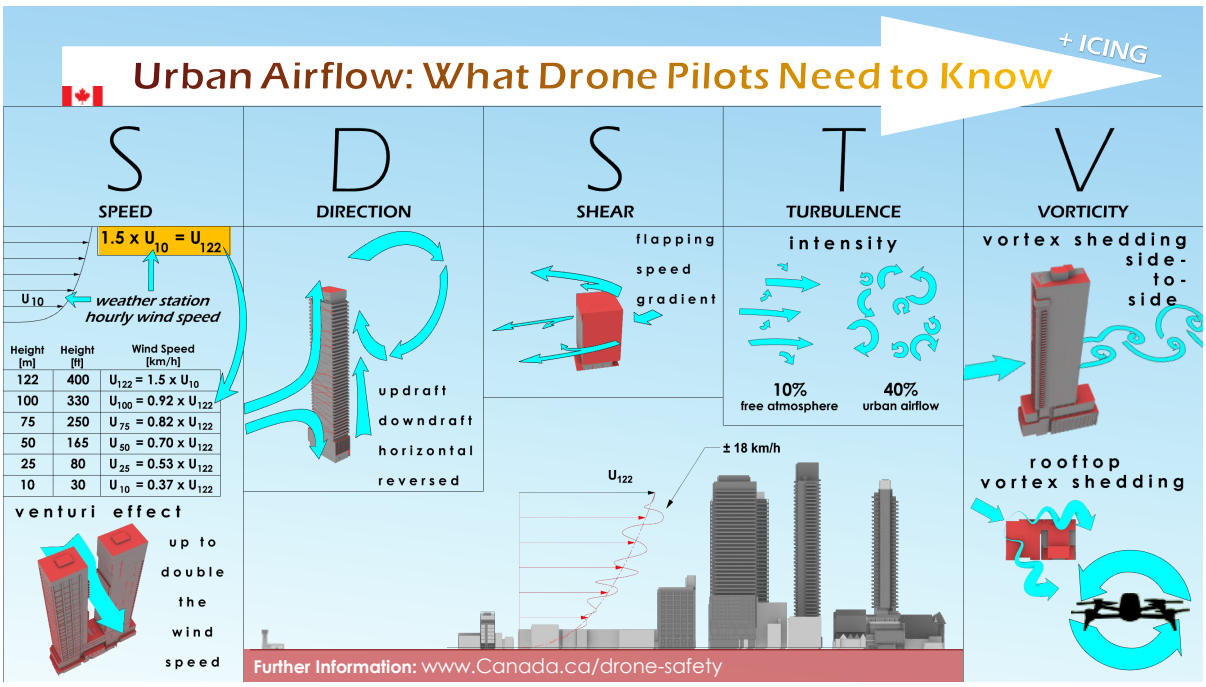

Figure 0.1: Video summary and RPAS urban airflow informational brochure.

This document includes the English language script and supporting background literature for the urban airflow information within the video and is designed as a companion to the video.

Contents

List of Figures

List of Tables

1. Introduction

The National Research Council of Canada (NRC) has a long-standing history of expertise in highly turbulent flow fields representative of airwakes caused by large structures found within urban centres. In 2019, the Transport Canada (TC) Remotely Piloted Aircraft Systems (RPAS) Task Force engaged the NRC to support RPAS pilot awareness for flight within urban flow fields. The current project aims to introduce RPAS pilots to the wide range of urban flow types within the urban environment as a first step towards safety measures in response to the rapid growth of RPAS operations within city centres.

1.1 Background - RPAS in the Urban Environment

For RPAS to operate safely in an outdoor environment, the effects that various forms of weather have on their control systems may be of concern. For a study on the impacts of weather on RPAS operations, Ranquist *et al.* (2016) has categorized the severity of weather into three categories including moderate, adverse and severe. Moderate weather conditions reduce visibility (fog, cloud cover, glare) but do not directly impact aircraft control. Adverse weather conditions (wind, atmospheric turbulence, temperature, humidity, rain, snow and ice) are conditions in which RPAS pilots are often expected to fly, that may impact aircraft control. Severe weather conditions (lightning, hurricane, tornado, hail) are commonly recognized as unsafe for flight. Under the general assumption that RPAS operators will not fly during severe weather conditions, and that moderate weather conditions do not pose a risk to RPAS control, the hazards from adverse weather are most likely to be the cause of RPAS accidents as a result of diminished aerodynamic performance and loss of control (Ranquist *et al.*, 2016).

Between 2003-2007, the Federal Aviation Administration (2010) reported that over 54% of accidents for small non-commercial manned aircraft were wind related. Ranquist *et al.* (2016) suggests that wind will affect RPAS more potently than the small manned aircraft because they are lighter in weight. Sustained and fluctuating wind forces acting on an RPAS have the potential to reduce performance including flight stabilization control, trajectory control, and speed (Watkins *et al.*, 2020). Along with reduced performance comes reduced flight endurance as a result of the RPAS requiring more thrust and therefore demand on battery power.

In addition to wind effects on RPAS, precipitation may also cause loss of control. Icing conditions can arise from precipitation when combined with freezing temperatures. Rain can freeze upon contact with the wings of a fixed-wing aircraft or the blades of a rotorcraft causing an increase in aerodynamic drag and a decrease in aerodynamic lift. For rotorcraft, the rotary motion assists in shedding ice, but asymmetric shedding can cause an imbalance due to uneven weight distribution and therefore vibration in the system (Brouwers *et al.*, 2010). A secondary effect of ice accretion on aircraft is a decrease in endurance due to an increase in required thrust caused by diminished performance and added weight (Benmeddour, 2020). The combination of propeller blade imbalance and an increase in required thrust can contribute to a

rapid decline in RPAS control.

On a calm day, losing control of an RPAS within the urban environment has an increased level of hazard in comparison to rural operations because the built structures within the city impose flight path restrictions making navigation difficult. Within a city, the RPAS flight plan must account for restrictions in pathways, loss of visual line of sight due to buildings, a limited number of emergency safe landing locations, and avoidance of populated areas. Adding to the complexity of navigating around the city structures are urban wind characteristics caused by interactions between wind and the structures.

Together, the urban wind characteristics are the flow features contained within a boundary around a city, termed the urban boundary layer (UBL). The characteristics of the UBL provide some context for the urban airflow features that may challenge RPAS operations.

1.2 Background - Urban Airflow

The UBL is part of the Earth's atmospheric boundary layer (ABL) and includes the vertical structure of the atmosphere in and above cities, where buildings present elements of high roughness due to their large vertical surfaces. The full depth of the UBL is nearly always in a state of turbulent motion (Lateb *et al.*, 2016). Within the UBL are sub-layers, as illustrated in Figure 1.1, which contain different air-flow characteristics.

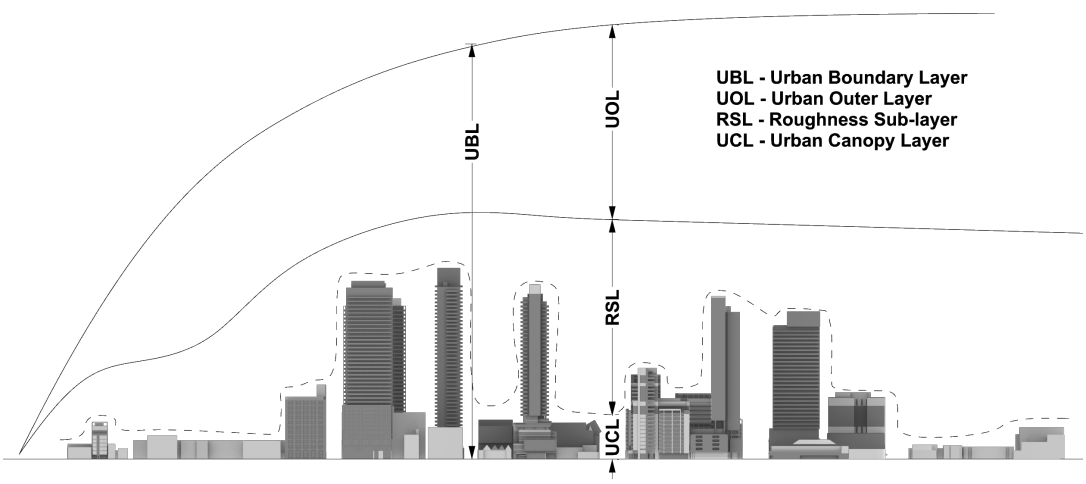

Figure 1.1: Sublayers of the urban boundary-layer.

The urban canopy sub-layer (UCL) includes the airflow from the ground up to the height of the buildings where a high variation in wind speed and turbulence are caused by blockage due to the high density of built structures where air is recirculated and diverted within street canyons. Above the UCL is the urban roughness sub-layer (RSL) which includes the region

where airflow above cities is affected by the landscape of the urban structures. Between the RSL and the full height of the UBL is an urban outer layer (UOL), where flow characteristics are mainly influenced by global winds which include atmospheric pressure distribution, surface friction and Corilois force (Lateb *et al.*, 2016). Within the UOL, the flow remains somewhat more turbulent than flow above the UBL, but does not have the magnitude of turbulence found in the UCL and RSL. Barlow (2014) estimates that the RSL within a city is between 2 and 5 times the mean building height, which implies that the RSL height is unique to the ratio of low-, mid- and high-rise buildings for each city.

1.2.1 Building Wakes

The wakes of buildings have two distinct wake regions, typical of bluff-bodies, where the mechanisms causing the flow characteristics differ. The bluff-body wake is typically defined by a near-wake region and a main-wake region as illustrated in Figure 1.2. The flow within the near-wake region is driven by the low-pressure at the leeward face, where flow is drawn into a highly turbulent low-pressure recirculation cavity. For tall buildings within a city, the near-wake region includes the flow within two building widths around the perimeter of the building where the recirculation diverts local street canyon flow. The main-wake is characterized by a momentum deficit, where the velocity deficit and turbulence intensity decay with downstream distance over the length of the main-wake, until the fluid properties have recovered to freestream levels. For buildings that are tall, where the wake is not blocked from dispersing downstream, the main-wake precipitates above the lower buildings with a distinct momentum deficit region which includes turbulent mixing (Hertwig *et al.*, 2019).

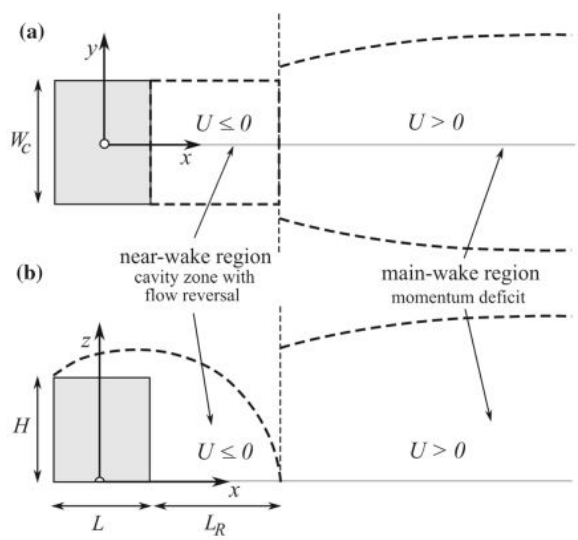

Figure 1.2: Bluff-body near-wake and main-wake regions: a) x-y plane - plan view, b) x-z plane - elevation view. Adapted from Hertwig *et al.* (2019).

1.2.2 Tall Buildings in Canadian Cities

For certain wind speeds and wind directions, the height of tall buildings within Canadian cities will cause turbulent wakes that are within the altitude restriction for small RPAS according to the Canadian Aviation Regulations (CARs) Part IX, which is 122 m (400 ft). Table 1.1 includes a list of major Canadian cities and the height range for the 20 tallest buildings in each.

Table 1.1: Range in height of the 20 tallest high-rise buildings per Canadian city (EMPORIS GMBH, 2020).

City	**Height Range** [m]	**Height Range** [ft]
Halifax	39 - 98	128 - 322
Quebec City	35 - 126	115 - 413
Montreal	130 - 226	427 - 742
Ottawa	87 - 148	285 - 486
Toronto	207 - 298	679 - 978
Calgary	152 - 247	499 - 810
Vancouver	126 - 201	413 - 659

For Quebec City and Halifax, the lowest heights of 35 m (115 ft) and 39 m (128 ft) are for buildings with 10 and 13 storeys, respectively, which represent mid-rise building heights. The lower maximum building height demonstrates that for smaller Canadian cities there are few high-rise buildings, highlighting the potential for a large range in UBL characteristics for Canadian cities.

Without detailed knowledge of specific airflow patterns for a Canadian city or the effect that the airflow has on an RPAS, a starting point for preparing RPAS users for urban wind conditions is to provide awareness of types of urban airflow and where/when that airflow type may occur.

Characteristics of Canadian cities, including building density and height heterogeneity, are important for the study of urban flow fields that are potentially hazardous to RPAS flight because the interaction of wind and structures determines the magnitude of the flow features. These flow features can be categorized into types, which are the focus of the RPAS safety awareness video information described in the following Chapter.

2. RPAS Urban Airflow Awareness Video: Script and Supporting Background Literature

To support Transport Canada (TC) promotion of safe operation of RPAS within the urban environment during the early stage of the regulatory development process, an RPAS user awareness video (Urban Airflow: What Drone Pilots Need to Know) on urban airflow characteristics was provided to TC by the NRC.

Considering that an RPAS flight path may traverse through all airflow types within an urban environment for Canadian city building heights, the objective of the RPAS urban airflow awareness video was to introduce all key urban airflow features caused by the presence of buildings that are expected to challenge operational speed and stability limitations. The specific objectives of the RPAS urban airflow awareness video are to:

- Provide an educational video focusing on wind characteristics within the urban environment that may challenge RPAS stability and control, and hence performance;
- Describe locations where the wind characteristics may occur with maximum magnitude;
- Warn users on loss of control due to icing; and
- Summarize the list of urban airflow characteristics in a graphical format for a future brochure that provides guidelines for anticipating the presence and estimating the magnitude of those characteristics.

The specific urban airflow characteristics expected to challenge RPAS operation control and limits include; speed (S), direction (D), shear (S), turbulence (T) and vorticity (V). These airflow characteristics define the acronym used in the video - SDSTV.

Although schematic images within the video were used to include as much information as possible, time restriction prevented a full explanation of each flow characteristic. Therefore this document includes background information used to determine the urban airflow characteristics generalized within the video.

The following sections present each video segment including introduction, urban airflow characteristic, and video summary of the English video script followed by supporting background information.

2.1 Introduction to the Video and Urban Airflow Acronym - SDSTV: Video Script

Info Script English (EN): *"This video provides awareness to RPAS users on the complex airflows within urban environments caused by interactions between the wind and the structures. Provided*

you are authorized to fly in this environment, the range of flow types shown in this video may be within the flight path of your remotely piloted aircraft. Changes in urban wind characteristics, due to the presence of buildings and structures, that may affect RPAS operational limits include: speed, direction, shear, turbulence, vorticity and icing."

2.2 Wind Speed - S

2.2.1 Wind Gradient: Video Script

Intro Script EN: *"Within the urban environment, wind speed will change depending on height and proximity to structures."*

Segway Script EN: *"Wind speed increases with height as the wind becomes less obstructed by the Earth's surface roughness, including trees and urban structures."*

Info Script EN: *"Global wind speed increases with height at an exponential rate. The rate of change in wind speed depends on terrain, and is therefore different for open country, found near most airports, in comparison to city- or urban-terrain."*

"To estimate the wind speed your RPAS will encounter at maximum altitude, a calculation can be made using a reference wind speed and the exponential relationship. For urban flight, using a reference wind speed measured at take-off location is not safe because the buildings in the city obstruct wind flow. Therefore, using a local weather station report is recommended, where mean hourly wind speeds, unobstructed by buildings, are measured at 10 m above ground. From the weather station report, we suggest calculating the speed at 122 m above ground, which is 1.5 times the weather station wind speed."

"'To estimate the wind speed closer to the ground, a calculation using the 122 m wind speed as a reference can be used if needed. Alternatively, for a quick guide, a height to wind speed ratio table will be provided at the end of this video."

2.2.2 Wind Gradient: Background

The wind speed within the ABL of the Earth, has been well defined by theoretical profiles, which model the increase of wind speed with height. The curvature of the theoretical profiles is dependent on the roughness of the Earth's surface and therefore changes with terrain type. A power-law curvature is a widely used and relatively simple method for modeling ABL wind speed over a wide range of terrain types as described by the following equation (Davenport, 1960; Kent *et al.*, 2018):

$$\frac{U}{U_{ref}} = \left(\frac{z}{z_{ref}}\right)^{\alpha} \tag{2.1}$$

where U is the wind speed at a distance, z, above the Earth's surface. U_{ref} is the known wind speed at a fixed reference height, z_{ref}, and α is the power-law exponent which varies with terrain type.

The power-law profile assumes a consistent mixing of surface turbulence which predicts a smooth transition of wind speed with respect to height. For urban locations where the wind has been blocked by structures, the wind does not follow the power-law profile within the height of a building wake. Figure 2.1 illustrates the impact of structures on a wind speed profile downwind of a building, where the wind is slower and much more turbulent in the wake of the building. The power law is sufficient within a city environment, but not within the near-wake of buildings.

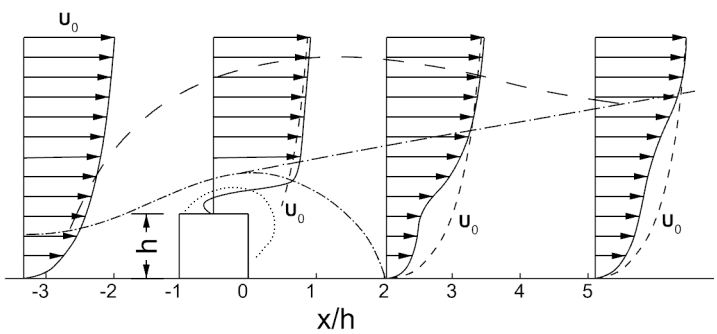

Figure 2.1: Wind speed profile around a cubical building. Adapted from Meroney (1982).

Due to the blockage of airflow and resulting change in wind characteristics within the urban canopy, locally measured street-level wind speeds cannot be used as a reliable reference wind speed for estimating wind speeds in the urban environment. Therefore using a reference wind speed from outside of, but near, the city such as from an airport weather station report is recommended. To estimate wind speed at various altitudes within the city using the airport weather report a two step process is required as illustrated in Figure 2.2. The following process assumes that a reference mean hourly wind speed reported at a weather station, such as an Environment Canada weather station, with a height of 10 m (33 ft) is used in the analysis.

For step 1, the reference mean hourly wind speed (U_{10}) from the airport location with an open terrain power law exponent (α) is used to determine the wind speed (U_x) at the cross-terrain reference height X. For step 2, U_x becomes the reference wind speed above the city. That reference wind speed can then be used in the power law with an urban terrain exponent (α) to make a second calculation of wind speed at lower heights (U_h) within the urban environment. National Building Code of Canada (NBCC) suggests a power law exponent of 0.40 for centres of large cities and 0.16 for open terrain where an airport is typically located (Simiu and Yeo, 2019).

For Canadian cities, determining a single reference height X is not straightforward. Theoretically, the height should be above a city's UBL to ensure the wind speed from the open terrain measured outside of the city is representative of the wind speed passing above the UBL. The difficulty with this method is that for Canadian cities the UBL height has a large range, as

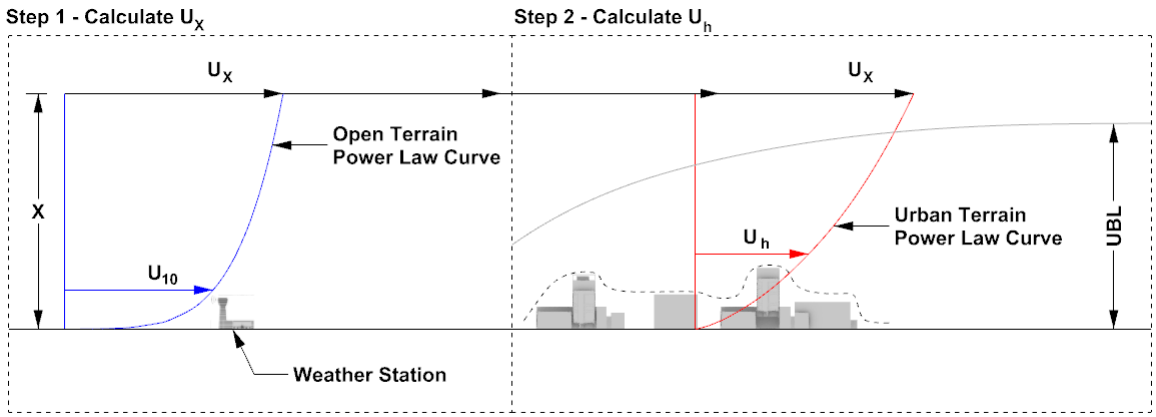

Figure 2.2: Power law profile using a cross-terrain reference height, X, above the UBL.

shown earlier in Table 1.1.

Figure 2.3 shows a scaled schematic of two urban elevation profiles representative of Canadian cities. The predicted UBL heights shown in Figure 2.3 are for a city with a high-rise density similar to Toronto and a smaller Canadian city without high-rise structures.

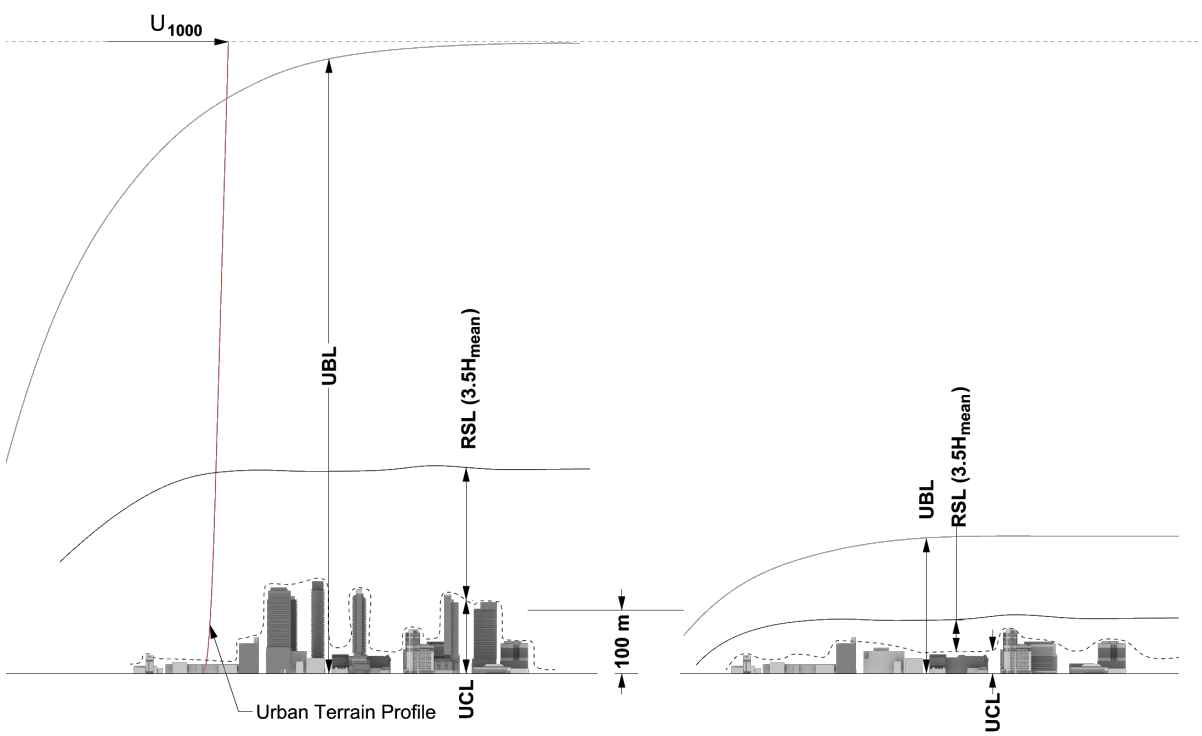

Figure 2.3: UBL, RSL and UCL height comparison for Canadian cities with and without high-rise buildings.

If the reference height is taken at a height that would be considered a typical UBL height of

approximately 1000 m (3300 ft) for a globally common city density (Barlow, 2014), the power law would under-predict the wind speed for lower heights within the smaller UBL of smaller Canadian cities, giving an unsafe estimate of wind speed at building heights. A more conservative method would be to use a lower reference height for which the effect of variation in city building density and height has less effect on the power law estimates.

Until studies have confirmed wind speed profile extremes for city densities and height heterogeneity consistent with Canadian cities, a safer approach would be to advise RPAS users to calculate the wind speed at the Canadian Aviation Regulations Part IX altitude limit for small RPAS (<25 kg), which is 122 m (400 ft), under the assumption that the wind speed at that height will be the upper limit of wind speed within their flight envelope.

In the future, local on-site wind measurements available to RPAS users from inner-city wind reports for a range of altitudes could be a more reliable method for estimating the real-world wind speed for a specific flight path. Currently, conservatively estimating the inner-city wind speed using the power-law method and the airport (open terrain) weather station mean hourly wind speed to determine the wind speed at 122 m (400 ft), will provide a safe and simple wind speed prediction as shown in the following. Step 1 - wind speed nearby the city:

$$U_{122} = U_{10}\left(\frac{122}{10}\right)^{0.16} = 1.5 \times U_{10} \tag{2.2}$$

where U_{122} is the estimated wind speed 122 m (400 ft) above ground and U_{10} is the mean hourly wind speed from a local weather station report, measured at 10 m (33 ft) above ground.

Step 2 - wind speed within the city:

$$U_h = U_{122}\left(\frac{h}{122}\right)^{0.40} \tag{2.3}$$

where U_h is the wind speed at flying height, h, and U_{122} is the wind speed calculated from Equation 2.2 ($1.5 \times U_{10}$).

To reduce calculation time, Table 2.1 provides the weather station wind speed correction to determine the wind speed at 122 m (400 ft) above ground and the additional urban power-law profile correction factors for a height below 122 m (400 ft). The wind speed at 2 m (7 ft) above ground has been included to emphasize the extremely low wind speed expected from a measurement at the height of a hand-held anemometer, which is 20% of the 122 m (400 ft) height wind speed. Table 2.1 also includes a factor for calculating the wind speed at the lower heights directly from the weather station report wind speed, U_{10}.

Table 2.1: Urban wind speed gradient estimation factors.

Height Above Ground (h), [m]	**Height Above Ground (h), [ft]**	**Urban Wind Speed correction for height (U_h), [km/h]**
122$^\diamond$	400	$U^\bullet_{122} = 1.5 \times U^\dagger_{10}$
100	330	$U^\star_{100} = 0.9 \times U_{122}$ (or $1.4 \times U_{10}$)
75	250	$U^\star_{75} = 0.8 \times U_{122}$ (or $1.2 \times U_{10}$)
50	165	$U^\star_{50} = 0.7 \times U_{122}$ (or $1.0 \times U_{10}$)
25	80	$U^\star_{25} = 0.5 \times U_{122}$ (or $0.8 \times U_{10}$)
10	30	$U^\star_{10} = 0.4 \times U_{122}$ (or $0.6 \times U_{10}$)
2	7	$U^\star_{2} = 0.2 \times U_{122}$ (or $0.3 \times U_{10}$)

$^\bullet$ Open terrain wind speed at 122 m (400 ft).
* Urban terrain wind speed calculation at height, h $\left(U_h = U_{122}\left(\frac{h}{122}\right)^{0.40}\right)$.
$^\diamond$ Maximum flying altitude for small RPAS (< 25kg)
† U_{10} represents the mean wind speed from an hourly weather report from a weather station at a height of 10 m (33 ft) located outside of, but near the city.

2.2.3 Urban Wind Gradient Variability: Video Script

Segway Script EN: *"Within the urban environment wind speed is also variable."*

Script EN: *"Within the urban wind gradient, speed can change quickly, by up to 18 km/h. The wind speed could be 10 km/h and then change to 28 km/h in a short period of time, so it is wise to limit your flight path to heights where wind speed is estimated to be 18 km/h <u>below</u> your RPAS sustained wind tolerance limit."*

2.2.4 Urban Wind Speed Variability: Background

Kent *et al.* (2018) used Doppler lidar measurements of wind speeds at heights of up to 2.5 times the mean building height (200 m (660 ft)) above a central London, UK location to compare the reliability of five commonly used methods to estimate the temporally- and spatially-averaged wind speed profile for an urban environment. Results found that with a fetch that is homogeneous, such as a sprawling suburban landscape, and a gradual increase in roughness towards the city centre, the power-law predicts the vertical wind speed profile well (Kent *et al.*, 2018), but for inner-city scapes during strong wind conditions where building heights within the fetch have large variability, the power-law estimates the mean hourly wind speed to within ± 5 m/s or 18 km/h (10 knots), which was approximately 50% of the measured wind speed. The author states that the ± 5 m/s (10 knot) variability was unavoidable, and likely due to the surface heterogeneity upwind of the measurement site, longitudinally and transversely.

Urban-model wind tunnel experiments by Hertwig *et al.* (2019) showed agreement with the Kent *et al.* (2018) field results, where measurements of the wind speed profile above a low- and mid-rise city-scape and within the RSL, showed large variation between measurement

sites, likely due to the variation in street and building configurations (Hertwig *et al.*, 2019).

In addition to the hourly variation in wind speed with height, gusting is also a factor, but has been excluded in the video due to a lack of supporting literature that would provide a simple factor that is independent of city density, building height heterogeneity, or upwind landscape characteristics.

2.2.5 Urban Wind Venturi Effect: Video Script

Segway Script EN: *"Due to disturbances caused by urban structures, wind speed can increase locally."*

Info Script EN: *"If the spacing between buildings restricts the path of the wind, the air flowing through the constriction may increase in speed, causing a venturi effect. The wind speed may increase by as much as double the speed of the upstream wind. This can occur at any building height including pedestrian level."*

2.2.6 Urban Wind Venturi Effect: Background

The urban wind venturi effect is caused by constriction in the path of the wind, including between closely spaced tall buildings or through openings within a facade. If the wind direction is parallel to streets with rows of buildings, the airflow is channeled along the street as illustrated in Figure 2.4 (Bailey *et al.*, 1997).

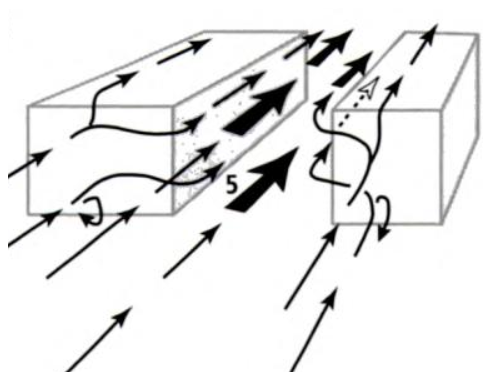

Figure 2.4: Illustration of a constriction jet between rows of buildings. Adapted from Bailey *et al.* (1997).

From wind tunnel experiments on modular models of urban density representing a hypothetical city, Cermak (1995) found that tall buildings adjacent to city street corridors caused a venturi effect for some wind directions. The experiment included configurations where the addition of rectangular building towers of 40 m (130 ft) tall were added to the top of a base building of 59 m (195 ft). With the addition of the 40 m (130 ft) buildings, whether they were spaced evenly or unevenly, the wind speed within the street corridor at a height of 99 m (325 ft) above ground, doubled in speed.

RPAS may encounter venturi flow along a flight path in addition to the strong vertical gradient and variability of urban wind speed.

2.3 Wind Direction - D

2.3.1 Wind Direction: Video Script

Intro Script EN: *"Urban airflow between and around structures can also change direction."*

Info Script EN: *"Tall buildings within a surrounding low-rise urban-scape redirect flow causing vertical and horizontal currents. Vertical flow includes updraft and downdraft. On the windward side of a tall building, downdraft causes street level flow to divert horizontally away from the building. Alternately, the low pressure zone on the leeward side draws horizontal flow towards the base of the building which converges into vigorous updraft. These wake features which include flow reversal and updraft can persist for the entire height of a tall building and the recirculation cavity driven by this motion, can extend downstream for up to twice the building height."*

2.3.2 Wind Direction: Background

The presence of high-rise buildings within an urban environment can cause wind direction to change at heights above and within the low- and mid-rise building canopy. The change in direction can include updraft, downdraft, zones with recirculation and vortices. Wind tunnel flow visualization results shown in Figure 2.5 from a study by Kuznetsov *et al.* (2016) on the influence of high-rise building height on distribution of wind pressure on low- to mid-rise buildings demonstrates the change in direction, or diversion, in urban airflow which includes updraft, downdraft and a recirculation cavity.

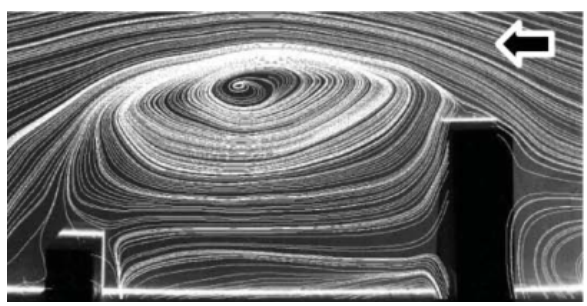

Figure 2.5: Illustration of building airflow diversion using particle image velocimetry by Kuznetsov *et al.* (2016).

A wind tunnel study by Hertwig et al (2019) measured the wake characteristics and airflow around a 134 m (440 ft) tall building surrounded by low-rise (up to 12 m (39 ft) in height) and mid-rise (up to 24 m (79 ft) in height) using 1:200 scaled models. The experimental testing showed that tall buildings within a surrounding low-rise urban-scape affect flow at street level as wind is redirected. On the windward face of the high-rise building, the downdraft increases

the street level horseshoe vortex causing an increase in divergence of horizontal flow through the street canyon. Alternately, the low pressure zone on the leeward side draws horizontal flow towards the base of the building which converges into strong updraft (Hertwig *et al.*, 2019).

From the same experimental results for airflow around the 134 m (440 ft) tall building, the height of the flow reversal in the near-wake recirulation zone was presented with respect to building height, H, and found to range between 0.56H and 0.63H for three different wind directions (Hertwig *et al.*, 2019), which is approximately 25 m (82 ft) above the roof height of the surrounding mid-rise buildings.

For a shorter high-rise, at 81 m (266 ft) tall, surrounded by low- to mid-rise buildings, the length of the recirculation zone was found to extend downstream for 0.13H to 0.78H (0.8 m (2.6 ft) to 50 m (164 ft) full scale). For low-rise buildings downstream of high-rise buildings, the influence of the reversed flow from the tall building will be present, but the strength of the flow reversal is weakened by the roughness of the surrounding low-rise buildings, reducing the length of the recirculation cavity. This effect is similar to results for isolated buildings, where elevated atmospheric turbulence levels have been shown to reduce the recirculation cavity length of the building wake (Hertwig *et al.*, 2019).

An RPAS operator may encounter an unexpected change in wind direction when downwind of buildings although weather reports show steady wind speed and direction.

2.4 Wind Wake Shear - S

Intro Script EN: *"Near building corners wind speed changes rapidly."*

2.4.1 Shear Layer Speed Gradient: Video Script

Segway Script EN: *"This airflow feature is known as a shear layer."*

Info Script EN: *"A shear layer is a narrow band of flow at the outer boundary of a building wake, where the outer side of the band is equal to unobstructed wind speed and the flow on the inner side is slowed by the presence of the buildings and is drawn into the highly turbulent recirculating flow. Shear flow will develop at the windward corners of the building, including the roof."*

"If the airflow has enough building length to reattach and form a recirculation bubble, a shear layer may also develop at the leeward corners."

2.4.2 Shear Layer Speed Gradient: Background

A shear layer is a band of flow with a steep velocity gradient that develops where flow separates from a bluff-body. The thick white streamline bands in Figure 2.6 show smoke visualization of the shear layers that have formed between the freestream flow and the separated flow

for a square cylinder. The incident angle between the oncoming smoke flow and the square cylinder for the case shown in Figure 2.6 is 15°, which causes a large separation angle on the upper corner of the cylinder producing a thin shear layer with an outer flow speed in excess of that of the freestream flow and an inner flow speed slowed by the adjacent low pressure zone. For the lower leading edge corner, the separation angle is small, which allows the flow to reattach to the cylinder and separate again at the trailing corner, forming another shear layer.

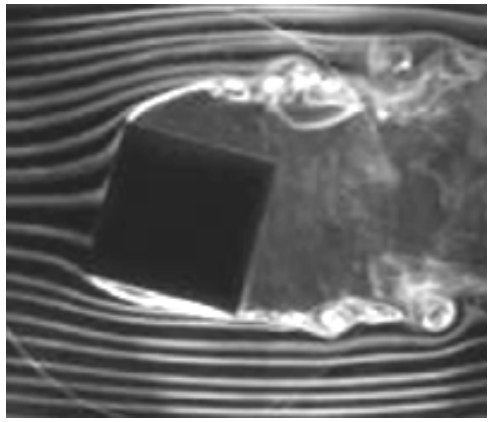

Figure 2.6: Visualization of shear layers for a square cylinder at a 15° incident angle. Adapted from (Sohankar *et al.*, 2015).

For buildings, reattachment of the flow, after the initial separation at the leading sharp corner, is influenced by the turbulence level in the atmosphere. An increase in turbulence reduces the length required for reattachment, which for a building side or top, increases the likelihood that a second separation at the trailing edge will occur. The trailing edge shear layer is thicker because the recirculation cavity is downstream of the building rather than beside it, causing less constriction on the shear layer width. Since global winds are always turbulent, Hunt (1971) suggests that unless a building is smaller in the wind-direction than in the cross-wind direction, the flow around a building likely includes a double separation on each side of the building and a wide shear layer.

Hertwig *et al.* (2019) used wind tunnel tests of a 1:200 scale model of London, UK, to investigate urban airflow characteristics including rooftop shear. From velocity profile measurements at the leeward side of the tall building (81 m (266 ft)), Hertwig *et al.* (2019) found a strong shear in the flow located at the height of the building. This indicated that the flow was separating from the downstream edge of the rooftop, and therefore reattaching to the roof after the initial leading edge separation. The results from Hertwig *et al.* (2019) are shown in Figure 2.7, where the open circles (no colour) denote the measurement location above the street directly adjacent to the tall building. The measured wind speed normalized by the free stream speed, $\frac{U}{U_{ref}}$, for a height relative to the building height, $\frac{z}{H_{81}}$, transitioned from -0.1 to 0.6 over a height of 0.8 to 1.0. The extreme change in wind speed shows a switch in direction, changing from reversed flow within the wake cavity to a positive streamwise direction that is half of the speed of the freestream flow. For the next measurement height of 1.1, the wind speed increased by 0.4 to a wind speed equivalent to the freestream flow. Although the measurement resolution does

not clearly define the thickness of the rooftop shear layer, the results demonstrate the extreme wind speed gradient that develops at the corners of buildings for a scaled model of a city.

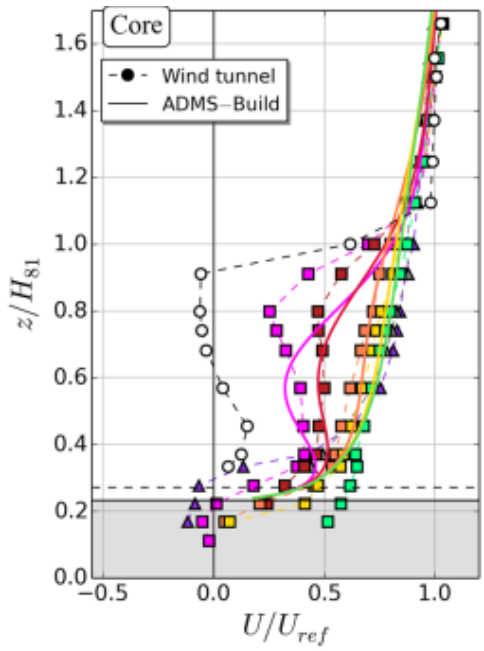

Figure 2.7: Wind speed profile downwind of a tall building (81 m (266 ft)) measured using a 1:200 model scale of London, UK, Adapted from (Hertwig *et al.*, 2019).

The effect of shear layers in the context of flight vehicles was investigated by Watkins *et al.* (2019). The location above a 43 m (141 ft) tall building resulting in the worst-case flight-relevant wind effect on two fixed-wind RPAS (32 kg and 109 kg) was identified using computational fluid dynamics (CFD) simulations and water-channel tests. It was found that passing through the leading-edge shear layer of the building while travelling in the same direction as the wind, caused the greatest disturbance due to a 15° change in angle of attack and a 50% increase in flight speed.

2.4.3 Shear Layer Flapping: Video Script

Segway Script EN: *"Shear layers are not a fixed feature."*

Info Script EN: *"They flap inward and outward as the wake shifts in time."*

"Passing through a shear layer may cause RPAS instability due to a shifting and uneven distribution of wind force across the aircraft."

2.4.4 Shear Layer Flapping: Background

The continual shift of turbulent structures in the wake of a building causes shear layers to fluctuate in time. As the wake motion causes the flow separation angles to change, the shear layers exhibit a flapping effect. As the shear layers comprise the outer boundary of the near-wake, observation of the the intermittent reattachment of separated flow on rooftops seen in various experimental studies (Hertwig *et al.*, 2019) demonstrates the fluctuation of near-wake airflow which includes shear layers.

For helicopter studies on pilot response to ship airwakes, it has been found that when the aircraft rotor size is comparable in size to the shear layers and vortical structures, the fluctuating forces and associated moments can cause increased difficulty in flying and station-keeping (Kaaira *et al.*, 2012). Considering the wide range in RPAS size from micro-quadrotor to flying taxi, the shear layer characteristics, including cross-stream width, speed gradient, proximity to buildings and flapping frequencies may be critical in determining RPAS flight control limitations.

2.5 Wind Turbulence - T

2.5.1 Turbulence Intensity: Video Script

Intro/Segway Script EN: *"RPAS instability can also result from high intensity turbulence within urban airflow."*

Info Script EN: *Atmospheric turbulence is the disorderly movement of eddies in the atmosphere. Atmospheric turbulence intensity is a measure of the fluctuation in wind speed caused by turbulence, in comparison to the average wind speed. The continuous change of airflow in both direction and speed causes rapidly changing forces on RPAS, which increase as the turbulence intensity increases. Within the urban environment, turbulence intensity can be <u>4 times</u> more severe than in the free atmosphere above open country.*

2.5.2 Turbulence Intensity: Background

Mechanical atmospheric turbulence found within the urban boundary layer is generated by the roughness of the city-scape and the wakes of high-rise buildings. Turbulence in the wake of a high-rise building contains unorganized eddies that are of a smaller scale than atmospheric turbulence and have a higher turbulence intensity (Hertwig *et al.*, 2019). Although the wake flow moves in a steady downstream direction, the flow contains a significant fluctuating component (Hunt, 1971).

For cities with large variability in building height, the high-rise building wakes that are above lower buildings may persist downstream for the same distance as an isolated building wake (Meroney, 1982) and are generally as wide as the high-rise building (Hunt, 1971).

With a change in wind direction the shape of the building wake may change, but the turbulence level within the wake remains high. Hansen and Cermak (1975) measured turbulence intensity, I_u, within the wake of a surface mounted rectangular block, representing a building, using a wind tunnel configuration with wind simulating the ABL over suburban terrain ($I_u = 10\%$). The building was oriented perpendicular and at a 47° incident angle to the wind. The results by Hansen and Cermak (1975), shown in Figure 2.8, found the wake turbulence intensity to be between 30% and 40% in excess of the ABL turbulence level ($I_u = 40\%$ and 50%) at roof height for up to 2.5 building heights downwind for both of the wind incident angles.

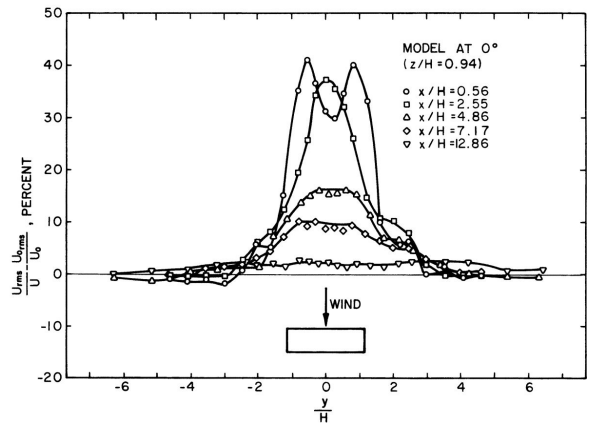

(a) Building wake turbulence intensity excess in the lateral plane for perpendicular winds.

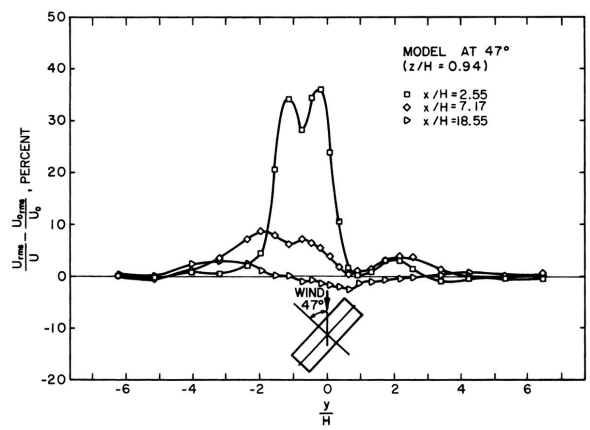

(b) Building wake turbulence intensity excess in the lateral plane for 47° winds.

Figure 2.8: Turbulence intensity excess in the wake of a model building. Adapted from Hansen and Cermak (1975).

The height of the highly turbulent wake above the rooftop has also been studied for exhaust plume dispersion models. Wilson (1979) used water channel experiments with a model building to define a method for estimating the height of highly turbulent regions above a roof, concluding that a reasonable estimation of turbulent wake height at the roof centreline, H_c, to

be:

$$H_c = 0.22R \; at \; x_c = 0.5R \tag{2.4}$$

where x_c is the distance along the roof at centreline from the leading edge and R is:

$$R = D_{small}^{0.67} \times D_{large}^{0.33} \tag{2.5}$$

where the D values are the small and large dimensions of the upwind face of the building.

Figure 2.9 illustrates the location of H_c and x_c with respect to a building roof, near-wake cavity, turbulence zone and roof wake boundary.

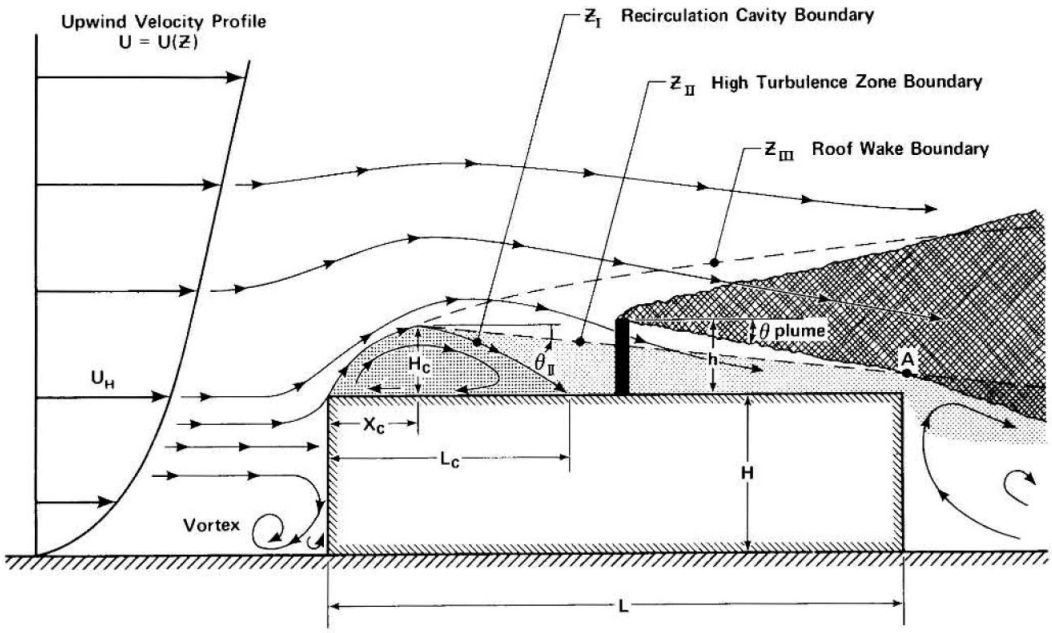

Figure 2.9: Turbulent wake zone for a building rooftop. Adapted from (Wilson, 1979).

The method by Wilson (1979) estimates that a high-rise of 100 m (328 ft) tall x 20 m (66 ft) wide would have a region of highly turbulent recirculating flow for up to 7.5 m (24.6 ft) above the roof at the roof centreline, 17.0 m (55.8 ft) downstream of the building face. For a mid-rise building of 34 m (112 ft) tall x 20 m (66 ft) wide, the results would be 5.3 m (17.4 ft) above the roof at 12.0 m (39.4 ft) downstream. Clearly this can represent challenges to an RPAS pilot attempting a vertical descent to land on the roof of a tall building.

The results found by Wilson (1979) also demonstrate the turbulence associated with urban roughness caused by the grouping of buildings with variation in rooftop size and height. The surface roughness caused by the differing heights of the low- and mid-rise buildings also adds turbulence intensity to urban airflow. Hertwig *et al.* (2019) found that the urban surface roughness, as a result of street spacing and building blockage, from low-rise (less than 12 m (39 ft) in height) and mid-rise (12 m (39 ft) to 24 m (79 ft) in height) buildings (without tall buildings in

place) changed the turbulence characteristics for a height extending up to 95 m (312 ft), with a peak in turbulent kinetic energy (TKE, k = $0.5(u'^2 + v'^2 + w'^2)$) and vertical momentum flux $\left(-\overline{u'^2 w'^2}\right)$ at a height twice the low-rise building height (27 m (89 ft) full scale). This finding places the extreme of the turbulent flow within the RSL of the UBL just above the rooftops of the mid-rise buildings.

A combination of the surface roughness of densely spaced low- and mid-rise buildings and the wakes of sparsely spaced high-rise buildings can create complex and highly turbulent structures within the urban flow field.

For objects moving through atmospheric wind, the turbulence intensity perceived by the object changes with the direction of motion of the object. The turbulence intensity in motion, J_u, is given in the following equation (Watkins *et al.*, 2006):

$$J_u = \frac{\sqrt{(u')^2}}{V_r}, where \quad V_r = \sqrt{(u + V_{RPAS})^2 + v^2 + w^2} \tag{2.6}$$

where u, v, w are the mean wind vector components, $\sqrt{u'}$ is the variation in the u component, and V_{RPAS} is the ground speed of the RPAS traveling in the same direction as u.

With an increase in the perceived u component caused by the motion of the object J_u is reduced, demonstrating that the direction and speed of the RPAS will alter the effects of the highly turbulent urban airflow on the aircraft.

2.6 Wind Vortices - V

2.6.1 Side-to-side Vortex Shedding: Video Script

IntroScript EN: *"Turbulence can also manifest in the form of building induced vortex shedding. The type of vortex shedding is dependent on wind direction and building orientation."*

Segway Script EN: *"Vorticity can develop in a side-to-side vortex shedding pattern."*

Info Script EN: *"The wind approaching some structures at some angles may cause counter-rotating wake-vortices that rotate about a vertical axis and are shed from the leeward building face in a side-to-side sequence. The size of the shed vortices is similar to the width of the building."*

2.6.2 Side-to-side Vortex Shedding: Background

Different wind directions cause different types of wake-vortex shedding from buildings. If the wind direction ranges from perpendicular to some oblique angle, with respect to a building face, bluff-body vortex shedding may occur (Barber *et al.*, 2020), where the counter-rotating wake-vortices rotate about a vertical axis and are shed side-to-side from the back face of the building. Building wakes with this type of shedding can have a length of up to seven times the building height (Meroney, 1982). This type of vortex shedding typically releases vortices that

are spatially similar to the bluff-body width, which in the urban environment is the building width.

Figure 2.10 shows a photograph of clouds in a bluff-body vortex shedding formation. The image illustrates the side-to-side vortex pattern and the size of the released vortices with relation to the bluff-body, which in this case is an island near Chile.

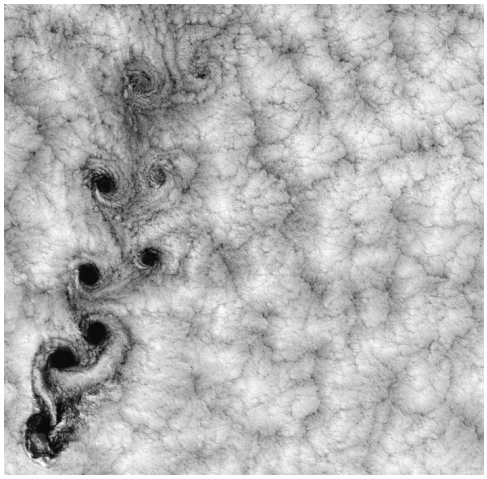

Figure 2.10: Cloud vortex shedding in the wake of Juan Fernandez Island. Sharp (2011).

2.6.3 Rooftop Vortex Shedding: Video Script

Segway Script EN: *"Coordinated vortices can also appear within rooftop wakes."*

Info Script EN: *"If the wind approaches the building face at an angle, two strong roof-top counter-rotating vortices emanate from the windward corner of the roof with a horizontal trajectory. Horizontal vortices can be a stability hazard to RPAS as they apply an overturning force to the aircraft, particularly if the vortex and RPAS are similar in size."*

2.6.4 Rooftop Vortex Shedding: Background

If the wind approaches the building face at oblique angles, two strong roof-top counter-rotating vortices emanate from the windward corner of the roof with a horizontal trajectory (Meroney, 1982). This type of vortex structure increases the main-wake length as the horizontal vortices may persist for 80 building heights downstream (Hansen and Cermak, 1975).

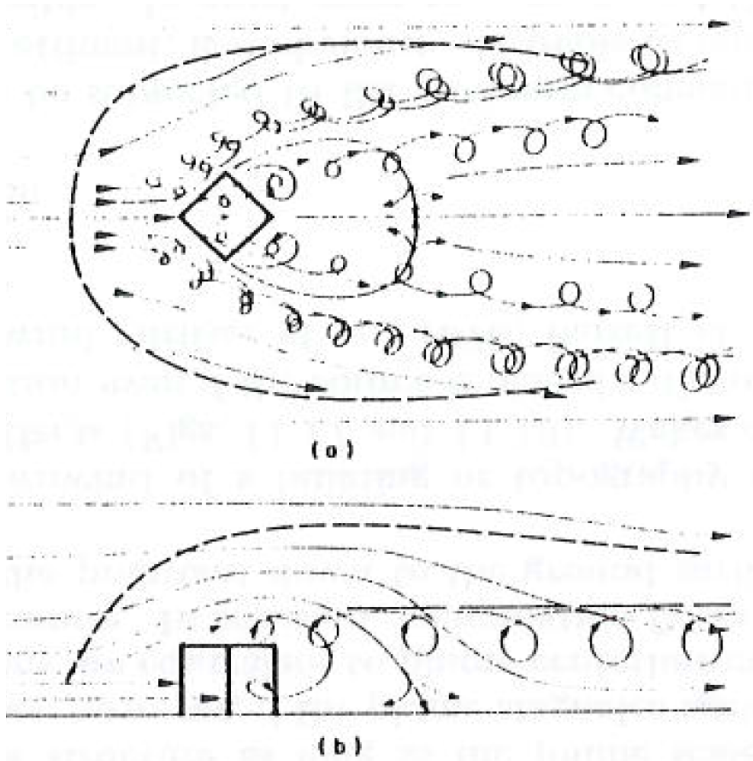

Figure 2.11: Fluid physics of wind flow around a square building for a 45° incident angle. Adapted from Meroney (1982).

Figure 2.11 illustrates the physics of the flow around a rectangular building for an incident wind angle of 45°. Image (a) illustrates the rooftop vortices that progress downwind from the

leading corner of the roof. Image (b) illustrates the horizontal path of the vortex structure as it moves downstream.

Loss of control of an aircraft due to an overturning moment caused by a vortex structure with horizontal trajectory shed from an upstream aircraft has been linked to vortex encounters causing aircraft instability, where the vortex strength and response of the encountering aircraft are directly proportional to the upstream aircraft size (Morky, 2003). Figure 2.12 illustrates the relationship of the vortex size to the overturning moment imposed on an aircraft of similar size. Rooftop edge vortices with a horizontal trajectory may pose an analogous hazard to RPAS as aircraft wake vortices do to small manned aircraft. The likelihood of flight disturbances on aircraft due to rooftop vortices is increased by the smaller size, and range in size, of remotely piloted aricraft, because the control and stability are scale- and aircraft-specific (Watkins *et al.*, 2020).

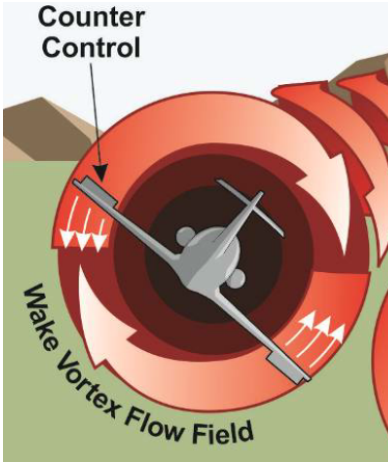

Figure 2.12: Vortex aircraft interaction stability hazard schematic. Adapted from the Federal Aviation Administration: Advisory Circular (2014).

2.7 Icing

2.7.1 Icing: Video Script

Intro Script EN: *"RPAS users must also watch for icing conditions."*

Info Script EN: *"In addition to operational hazards due to the complex airflow within the urban environment, for cold conditions, instabilities caused by ice accretion impact the performance of rotor blades, potentially making it impossible for the RPAS to fly. For rotor diameters under 350 mm, the quick build-up of ice can reduce thrust by 50% in less than 30 seconds."*

2.7.2 Icing: Background

Information included in the video on the impacts of icing on rotor thrust was referenced from a NRC report by Benmeddour (2020). The report documents testing of ice accretion on three composite propellers with varying diameter (254 mm (10 in), 305 mm (12 in) and 356 mm (14 in)) and constant pitch, typical of small RPAS, to examine the time taken to reduce thrust by 50%. The tests configurations included a 15 m/s (29 knots) wind speed for propeller rotational speeds of 8000 RPM and 9000 RPM and a range in ice growth parameters for a constant -12° C temperature. Within the blade diameter range and ice growth parameters, thrust was reduced by 50% with exposure times ranging from 30 s and 450 s.

2.8 Video Summary

2.8.1 Video Summary Script

Info Script EN: *"Icing conditions are a consideration along with speed, direction, shear, turbulence and vorticity, SDSTV, as each adds potential weather-induced hazards within the urban environment that RPAS users should be aware of when planning or maneuvering through a flight path. To reduce risk of adverse wind effect on your RPAS operations, flying in calm conditions is advised, which is more likely in mornings and evenings."*

"This urban airflow awareness video has been presented to you by Transport Canada's RPAS Task Force, with support from the Aerodynamics Lab at the National Research Council of Canada and RWDI. For related RPAS information go to the Transport Canada website at www.canada.ca/drone-safety."

2.8.2 Video Summary Image Information

Figure 2.13 is a copy of the image at the conclusion of the video. The image summarizes characteristics presented within the video of urban airflow characteristics including: speed, direction, shear, turbulence and vorticity (SDSTV). The generalized magnitudes and descriptions of urban airflow features in the summary image include:

- Wind speed at 122 m (400 ft, maximum altitude for a small RPAS) equals $1.5 \times U_{10}$, where U_{10} is the mean hourly wind speed reported by a weather station at a height of 10 m (33 ft) from a nearby airport.
- Wind speed estimations at heights below 122 m (400 ft) and within the urban environment (reference table).
- Wind speed may vary at any height by 18 km/h (10 knots) in the urban environment.
- Wind speed may double within constricted paths - venturi effect.
- Wind direction changes significantly around tall buildings forming currents of updraft, downdraft, horizontal flow and flow reversal.
- Wind shear layers develop at building corners and consist of a strong velocity gradient.
- Wind shear layers flap inward and outward.
- Atmospheric turbulence intensity can be up to 40% within the urban environment.
- Building induced vortices can shed in a side-to-side sequence where the vortex size is similar to the building width.
- Building induced vortices with a horizontal trajectory can develop at rooftop corners.

The format of the summary image is intended to be useful for conversion to a brochure.

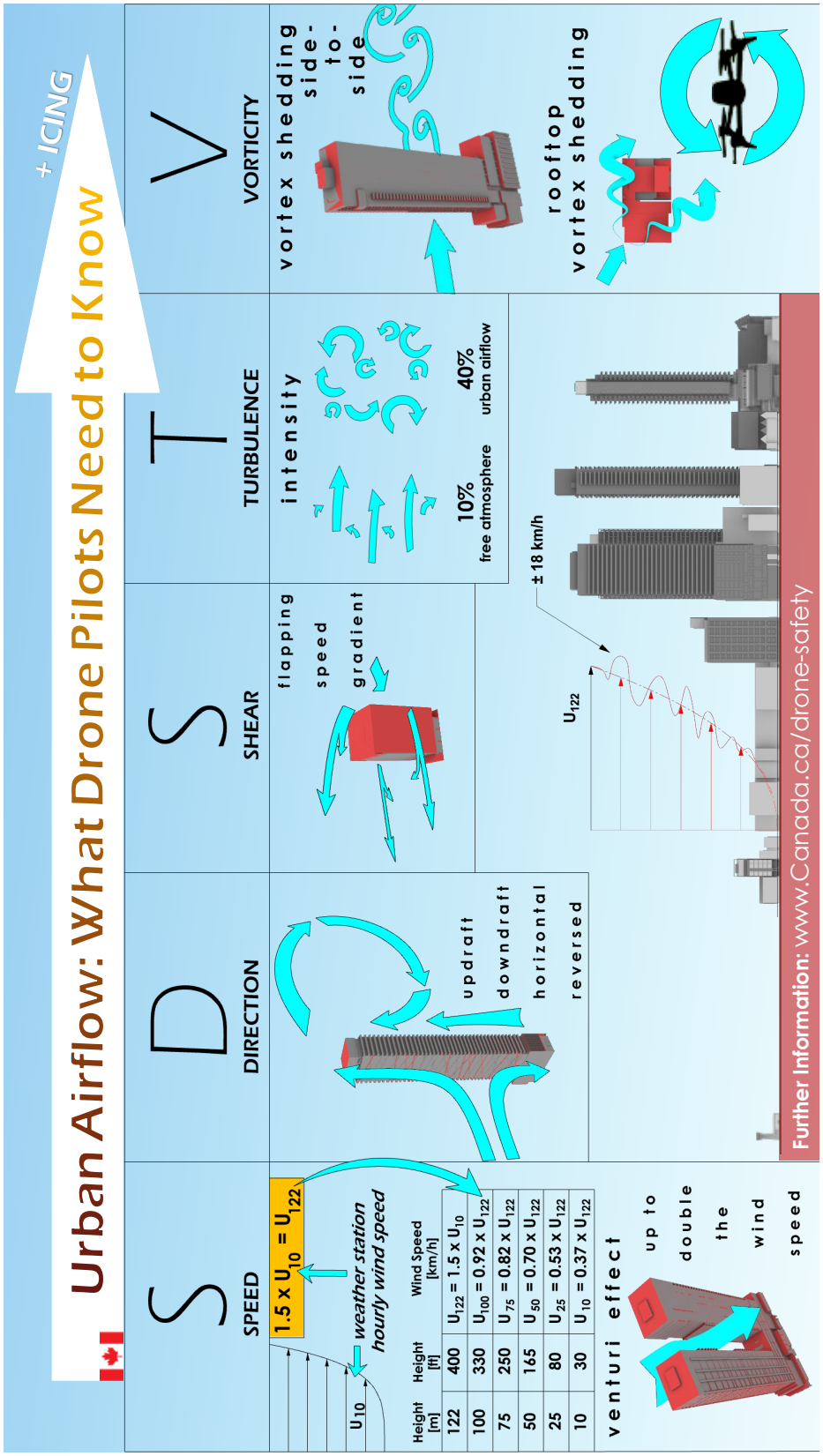

Figure 2.13: Video summary and RPAS urban airflow informational brochure.

References

Bailey, W. G., Oke, T. and Rouse, W. R. (1997), *The Surface Climates of Canada*.

Barber, H., Wall, A., Lee, R., McTavish, S. and Thornhill, E. (2020), "Experimental investigations into the effect of at-sea conditions on ship airwake characteristics," Submitted to Journal of Wind Engineering and Industrial Aerodynamics.

Barlow, J. F. (2014), "Progress in observing and modelling the urban boundary layer," Urban Climate, **10**, pp. 216–240.

Benmeddour, A. (2020), "Investigation of Tolerance for Icing of Small UAV Rotors/Propellers Phase 2," No. LTR-AL-2020-0053, *National Research Council Canada*.

Brouwers, E., Palacios, J., Smith, E. and Peterson, A. (2010), "The Experimental Investigation of a Rotor Hover Icing Model with Shedding," *66th Forum of the American Helicopter Society*, American Helicopter Society International, Inc.

Cermak, J. E. (1995), *Wind Climate in Cities*, Kluwer Academic Publishers.

Davenport, A. (1960), "Wind Loads on Structures," No. 88, *National Research Council of Canada Division of Building Research*.

EMPORIS GMBH (2020), *Statistics: Tallest Buildings*, https://www.emporis.com/statistics/tallest-buildings.

Federal Aviation Administration (2010), *Weather Related Aviation Accident Study 2003-2007*, https://www.asias.faa.gov/i/studies/2003-2007weatherrelatedaviationaccidentstudy.pdf.

Federal Aviation Administration: Advisory Circular (2014), *Aircraft Wake Turbulence*.

Hansen, C. A. and Cermak, J. (1975), "Vortex-containing wakes of surface obstacles," No. 29, *Colorado State University*.

Hertwig, D., Gough, H. L., Grimmond, S., Barlow, J. F., Kent, C. W., Lin, W. E., Robins, A. G. and Hayden, P. (2019), "Wake characteristics of tall buildings in a realistic urban canopy," Boundary-Layer Meteorology, **172**, pp. 239–270.

Hunt, J. (1971), "The effect of single buildings and structures," Phil. Trans. Roy. Soc. Lond. A., pp. 457–467.

Kaaira, C. H., Wang, Y., Padfield, G. D., Forrest, J. S. and Owen, I. (2012), "Aerodynamic Loading Characteristics of a Model-Scale Helicopter in a Ship's Airwake," Journal of Aircraft, **49**.

Kent, C. W., Grimmond, C., Gatey, D. and Barlow, J. F. (2018), "Assessing methods to extrapolate the vertical wind-speed profile from surface observations in a city centre during strong winds," Journal of Wind Engineering & Industrial Aerodynamics, **173**, pp. 100–111.

Kuznetsov, S., Butova, A. and Pospisil, S. (2016), "Influence of placement and height of high-rise buildings on wind pressure distribution and natural ventilation of low- and medium-rise buildings," International Journal of Ventilation, **15**, pp. 253–266.

Lateb, M., Meroney, R., Yataghene, M., Fellouah, H., Saleh, F. and Boufadel, M. (2016), "On the use of numerical modelling for near-field pollutant dispersion in urban environments - A review," Environmental Pollution.

Meroney, R. N. (1982), *Turbulent Diffusion Near Buildings*, Elsevier Scientific Pub. Co., Amsterdam.

Morky, M. (2003), "Hazard of wake vortex encounters in crosswind shear," Number AIAA 2003-378.

Ranquist, E., Steiner, M. and Argow, B. (2016), "Exploring the range of weather impacts on UAS operations," *18th Conference on Aviation, Range, and Aerospace Meteorology*.

Sharp, N. (2011), *Island Vortex Street*, https://fyfluiddynamics.com/2011/05/the-von-karman-vortex-street-is-a-series-of/.

Simiu, E. and Yeo, D. (2019), *Wind Effects on Structures: Modern Structural Design for Wind*, 4th ed., John Wiley & Sons.

Sohankar, A., Mohagheghian, S., Dehghan, A. and Dehghan Manshadi, M. (2015), "A smoke visualization study of the flow over a square cylinder at incidence and tandem square cylinders," Journal of Visualization, **18**, pp. 687–703.

Watkins, S., Burry, J., A., M., Marino, M., Prudden, S., Fisher, A., Kloet, N., Jakobi, T. and Clothier, R. (2020), "Ten questions concerning the use of drones in urban environments," Building and Environment, **167**.

Watkins, S., Milbank, J., Loxton, B. and Melbourne, W. (2006), "Atmospheric Winds and their Implications for Microair Vehicles," AIAA Journal of Aircraft, **44**, pp. 2.

Watkins, S., Mohamed, A. and OL, M. (2019), "Flight-Relevant Gusts: Computation-Derived Guidlines for MAV Ground Test Unsteady Aerodynamics," AIAA Journal of Aircraft.

Wilson, D. J. (1979), "Flow patterns over flat-roofed buildings and application to exhaust stack design," ASHRAE Transact, **85 (Part 2)**, pp. 284–295.